CrossMark

Amperometric determination of hydroquinone and catechol using a glassy carbon electrode modified with a porous carbon material doped with an iron species

Wei Huang [1] · Ting Zhang [1] · Xiaoya Hu [1] · Yang Wang [1] · Jianmin Wang [2]

Abstract

A porous carbon material doped with an iron species (Fe/PC) was prepared by carbonizing a mixture of zeolitic imidazolate framework-8 in the presence of iron(II) ions. The resulting material was characterized by X-ray diffraction, nitrogen adsorption isotherms, transmission electron microscopy, and by Raman and X-ray photoelectron spectroscopy. Fe/PC was the deposited on the surface of glassy carbon electrode (GCE) to obtain a sensor for amperometric determination of phenolic compounds. The unique catalytic activity, good electrical conductivity and hierarchical structure of the Fe/PC composite results in good electrooxidative activity towards hydroquinone (HQ; typically at 44 mV) and catechol (CC; typically at 160 mV). Under optimal conditions, the amperometric responses are linear in the range from 0.1 to 120 $\mu mol \cdot L^{-1}$ for HQ, and from 1.0 to 120 $\mu mol \cdot L^{-1}$ for CC. The respective detection limits are 14 and 33 $nmol \cdot L^{-1}$. The sensor is highly selective against potential interferents and was successfully applied to the determination of HQ and CC contents in (spiked) water samples.

Introduction

As important isomers of phenolic compounds, hydroquinone (HQ) and catechol (CC) always coexist in the pharmaceutical, fine chemicals, foods, cosmetics, and photography industries and so on [1, 2]. Because of their low degradability and high toxicity, they are not only harmful to the human health, but also cause serious environmental pollution. Both of those two compounds are listed as the significant environmental pollutants by the European Union (EU) and the US Environmental Protection Agency (EPA) [3]. For this reason, extensive research has been focused on the development and exploitation of analytical devices for the detection, quantification, and monitoring of HQ and CC levels.

Electrochemical analysis, possessing the advantage of fast response, low cost and simple operation, was widely used in the determination of various target analytes with electroactive group [4–6]. However, direct detection of HQ and CC using the bare electrode is difficult because the overlap of the isomer oxidation-reduction peaks. To solve this problem, the development of novel electrode materials for the simultaneous determination of HQ and CC with excellent sensitivity is important. Various carbon based electrode materials have been utilized to promote the electron transfer rate and improve the selectivity of sensors [7–9]. Among them, porous carbon holds great potential in the field of electrochemistry not only to their unique physical and chemical properties but also to their wide availability [10, 11].

✉ Yang Wang
wangyzu@126.com

Jianmin Wang
jmwang@tmmu.edu.cn

[1] School of Chemistry and Chemical Engineering, Yangzhou University, Yangzhou 225002, China

[2] State Key Laboratory of Trauma, Burns and Combined Injury, Institute of Surgery Research, Daping Hospital, Third Military Medical University, Chongqing 400042, China

Metal-organic-frameworks (MOFs), which are a new type of crystalline porous materials with multiple functionalities, have received great attention. Due to the different topological structures and significant amount of carbon source, MOFs are promising precursors for the production of highly porous carbon materials [12, 13]. For instance, a series of Co-MOFs-derived dual metal and nitrogen codoped carbon catalysts were investigated, which delivered excitingly high ORR activity, even comparable to that of Pt/C catalyst [14]. Although the MOFs derived porous carbon have been destined to be promising materials for energy storage, carriers for drug delivery systems, and contamination removal [15–17], the using of MOFs derived porous carbon as electrode materials for biomolecule detection is still a challenge till now.

With the above background, we report the synthesis, characterization and analytical characteristics of iron species doped zeolitic imidazolate frameworks (ZIFs) derived porous carbon materials. Its application for the development of a novel electrochemical sensor was reported for the first time for the simultaneous detection of HQ and CC. The electrochemical sensing characteristics were examined by cyclic voltammetry and differential pulse voltammetry in detail. The accurate determination of HQ and CC for real samples analysis demonstrated that MOFs derived metal doped porous carbon was a promising material for electrochemical biosensor applications.

Materials and methods

Materials and reagents

Iron (II) chloride tetrahydrate (FeCl$_2$ · 4H$_2$O) and 2-Methylimidazole (MeIm) were purchased from Aladdin-Reagent (Shanghai, China, www.aladdinreagent.com). Zinc nitrate hyexahdrate (Zn(NO$_3$)$_2$ · 6H$_2$O), methanol, hydroquinone, catechol, N, N-Dimethylformamide (DMF) and other chemicals were purchased from Sinopharm Chemical Reagent (Shanghai, China, www.sinoreagent.com) and all of them were analytical grade. Phosphate buffer was prepared by mixing the stock solution of 0.1 mol · L^{-1} NaH$_2$PO$_4$ and 0.1 mol · L^{-1} Na$_2$HPO$_4$ and adjusting the pH at 7.0 with 0.1 mol · L^{-1} H$_3$PO$_4$ or 0.1 mol · L^{-1} NaOH solution. Double deionized water (18 MΩ cm) was prepared by Milli-Q water purification system (Millipore, Bdfedford, MA, USA).

Apparatus

A CHI852C electrochemical workstation (Chenhua Instrument, Shanghai, China) was used for voltammetric measurements with a three-electrode system. The working electrode was the Fe/PC modified glassy carbon electrode (GCE) with a diameter of 3 mm. The counter electrode was a platinum wire and the reference was an Ag/AgCl (3 M KCl) electrode. The powder X-ray diffraction (XRD) patterns were collected with a Cu Kα (λ = 1.5406 Å, 40 KV, 40 mA) D8 Advance X-ray diffractometer (Bruker Co., Germany) from 5° to 80°. The Raman spectra were measured at room temperature through an In Via Laser confocal Raman microscope (Renishaw, UK) with an excitation of 633 nm. The transmission electron micrograph (TEM) images were obtained using a Philips Tecnai-12 (Netherland) operated at 120 KV. The X-ray photoelectron spectroscopy data were collected using ESCALAB 250Xi X-ray photoelectron spectroscopy (Thermo Scientific, America). Specific surface area (BET) was measured by Micromeritics ASAP 2020 HD88 physical adsorption instrument automation (America) by N$_2$ sorption at 77 K.

Construction of the modified electrodes

The synthesis of iron doped porous carbon (Fe/PC) was shown in Electronic Supplementary Material. The bare GCE was gently polished manually with 0.3 and 0.05 μm alumina slurry to obtain a fresh surface and cleaned successively with ethanol and double distilled deionized water by sonication for 2 min, respectively, finally, dried in N$_2$ blowing. After cleaning, 1.0 mg Fe/PC was ultrasonically dispersed into 1.0 mL DMF to produce a homogeneous solution. 5.0 μL Fe/PC solution was placed onto the GCE surface, and the solvent was allowed to evaporate at room temperature in the air. In addition, bare GCE and PC/GCE were also prepared in the similar way.

Operating procedure

The determination of HQ and CC was performed by means of differential pulse voltammetry (potential range: −0.3 - 0.6 V; increment: 4 mV; amplitude: 50 mV; pulse width: 0.2 s; sampling width: 0.02 s; pulse period: 0.5 s). The samples were determined directly or suitably diluted to draw the sample concentration within the linear range. 10 μL sample solution was transferred to a three-electrode cell and dissolved with 10 mL 0.1 mol · L^{-1} phosphate buffer (pH 7.0). All experiments were performed at room temperature.

Results and discussion

Choice of materials

Porous carbons are considered as efficient materials to enhance the performance of electrochemical sensors. To date, many efforts have been made towards the preparation of porous carbon with MOFs. This is not only because MOFs can act as both template and carbon precursor, but also due to their

potential physical and chemical functions. The ZIF-8, consisted of imidazolate linkers and Zn^{2+} ions, has an intersecting pore structure and high surface area, and compared to other organic precursor, still is low toxic and low cost [18, 19]. Hence, it was commonly used for the preparation porous carbon and integration with other materials. In addition, the introduction of iron species can promote the in situ formation of porous carbon, and also offer abundant catalytic sites to improve electrochemical activity. More importantly, the iron species doped porous carbon shows excellent catalytic activity and durability in acidic solutions [20]. Therefore, ZIF-8 was used as the representative precursor to synthesis iron species doped porous in this work.

Characterization of synthesized materials

The prepared material phase purity and crystal structure of ZIF-8 was characterized by powder XRD pattern. As shown in Fig. S1, each diffraction peak pattern of the prepared ZIF-8 are consistent with the previous results [20], indicating that the porous framework was formed successfully with high crystallinity. Although the stability of most MOFs materials in aqueous media remains a major concern for their further applications, the results indicate that a low level of iron species doping process did not destroy the ZIF-8 framework structure. All the diffraction peaks of Fe/ZIF-8 are consistent with the XRD spectra of the ZIF-8, clearly demonstrating the preservation of the ZIF-8 structure. Furthermore, with the doping of iron species into ZIF-8, the color of Fe/ZIF-8 varied from white to orange, also demonstrating that iron species were successfully doped into ZIF-8. After carbonization in the nitrogen atmosphere, both ZIF-8 and Fe/ZIF-8 were converted to PC and Fe/PC. The XRD patterns of PC and Fe/PC occurring at 25° and 44° corresponds to the (002) and (101) graphite carbon diffractions, respectively (Fig. S2) [21]. It is also found that Zn and iron characteristic peaks are not present in the XRD patterns of PC and Fe/PC. This may be due to the fact that most of zinc metal (with its boiling point of 908 °C) was reduced by carbon and then vaporized carbonization. The iron species are probably incorporated into carbons or removed during acid leaching [19, 22].

The morphologies of the ZIF-8 products were investigated through TEM. As shown in Fig. 1a and b, the synthesized pure ZIF-8 shows a typical hexagonal ZIF-8 crystal structure with a diameter around 100 ± 10 nm. After doping a certain amount of iron ions, the average diameters increase to about 150 ± 15 nm. This proved that iron doped ZIF-8 materials were formed by the addition of single monomeric MeIm and solvated Zn^{2+} and Fe^{2+} species. Although the materials inherited their original morphology after carbonized at 900 °C for 5 h, the pyrolysis of organic components at high temperature makes the surfaces of the original frame structure become wrinkled (Fig. 1c and d).

All details about nitrogen isothermal adsorption/desorption (Fig. S3), pore size distribution (Fig. S4), Raman spectra (Fig. S5), and XPS survey spectra (Fig. S6) are mentioned in Electronic Supplementary Information.

## Sensing properties of HQ and CC sensor

The electrochemical behaviors of HQ and CC on bare GCE, PC/GCE and Fe/PC/GCE electrodes were studied by cyclic voltammetry in phosphate buffer (pH 7.0). As shown in Fig. 2, two weak reduction peaks are observed at the bare GCE as well as a weak overlapping oxidation peak, indicating that the electrochemical activity of HQ and CC is low on the bare GCE. Two pairs of separation redox peaks with oxidation peaks at 0.129 V for HQ and 0.235 V for CC, and reduction peaks at 0.085 V for HQ and 0.193 V for CC appear on the surface of PC/GCE. The appearance of sensitive redox waves and the enhanced peak currents suggest that HQ and CC can be easily distinguished at PC/GCE. The increase in the peak intensities can be attributed to the relative large surface area and micro- and mesoporous structure of PC and the presence of nitrogen. ZIF-8 contains a rich nitrogen source in imidazolate ligands, which can donate extra electrons that increase the electronic conductivity [23]. Compared with bare GCE and PC/GCE, Fe/PC/GCE exhibits two pairs of distinguishable redox peaks with largest currents. The oxidation peak currents for HQ and CC are 51.3 and 47.0 μA, and the reduction peak currents are −63.2 and −41.6 μA. The reason for the improved performance may be due to the presence of iron species in the PC, which can facilitate the mass transfer during the electrochemical catalytic process and possess strong electrocatalytic activity to the electrooxidation and electroreduction of HQ and CC. In this work, different amounts of $FeCl_2 \cdot 4H_2O$ (0.04, 0.12, 0.2, and 0.4 mmol) were used to synthesize iron doped porous carbon. The results revealed that the current response of HQ and CC increased with the concentration of $FeCl_2 \cdot 4H_2O$ up to 0.12 mmol and then decreased at higher $FeCl_2 \cdot 4H_2O$ concentration. Probably because larger amounts of iron species will block the porous channel and cover the active surface of the material, leading to the decrease of the electrode surface area and current response. Thus, 0.12 mmol of $FeCl_2 \cdot 4H_2O$ was chosen for composites preparation.

The following parameters were optimized: (a) Sample pH value; (b) Scan rate. Respective data and Figures are given in the Figs. S7 and S8. We found the following experimental conditions to give best results: (a) A sample pH value of 7.0 (b) scan rate of 100 mV · s^{-1}.

Differential pulse voltammetric determinations

As shown in Fig. 3, differential pulse voltammetry was carried out to detect HQ and CC simultaneously by keeping the

Fig. 1 TEM images of ZIF-8 (a), Fe/ZIF-8 (b), PC (c), and Fe/PC (d)
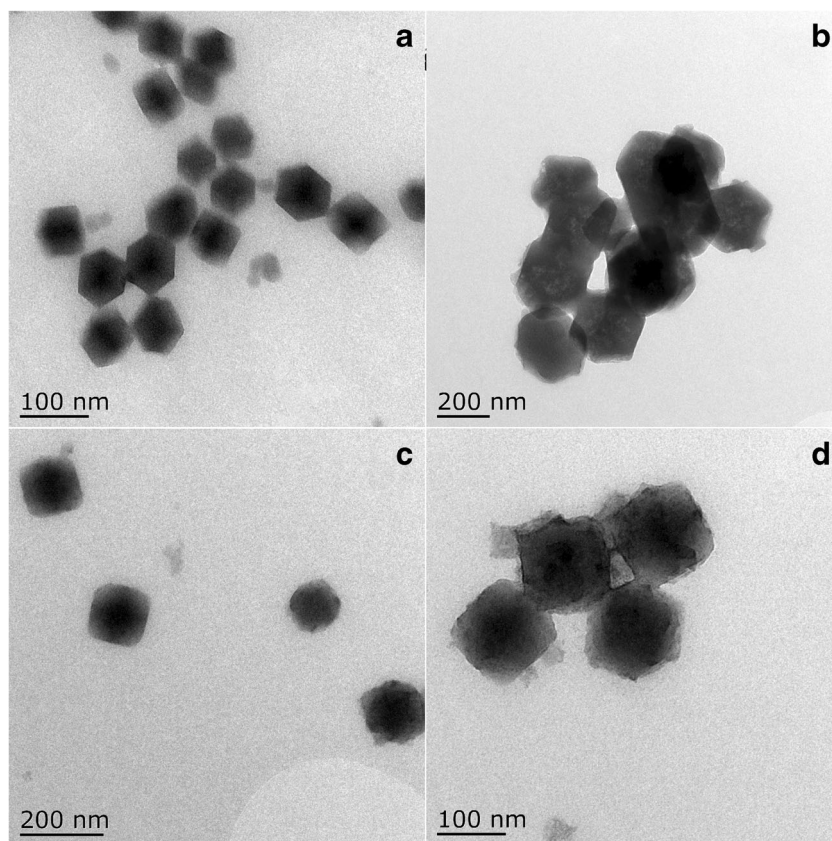
concentration of one component constant at 10.0 μmol · L^{-1} and increasing the concentration of other one under the optimal conditions. The peak current data were obtained at a working voltage of 44 mV (vs. Ag/AgCl) for HQ and 160 mV (vs. Ag/AgCl) for CC at a scan rate of 100 mV · s^{-1}. Detection limits for HQ and CC was calculated using 3σ/s definition, where σ is the standard deviation of the blank signals and s is the slope of the calibration curve. It can be noticed that the peak currents increase linearly with the increase in the concentration of the target molecule. For HQ,
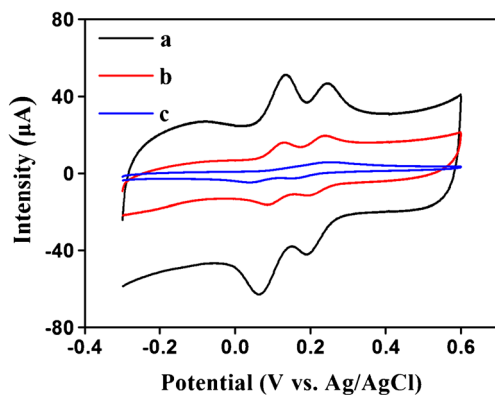
the relationship between peak currents and HQ concentration is in the range of 0.1–120 μmol · L^{-1}, and the linear equations of HQ are I_{pa} (μA) = 1.062 C (μmol · L^{-1}) + 1.064 (0.1–20.0 μmol · L^{-1}, R = 0.9996) and I_{pa} (μA) = 0.3721 C (μmol · L^{-1}) + 15.53 (20–120 μmol · L^{-1}, R = 0.9992). The limit of detection (LOD) was calculated to be 14 nmol · L^{-1}. Similarly, the anodic peak current is proportional to the concentration of CC from 1.0 to 120 μmol · L^{-1}. The linear equations are I_{pa} (μA) = 0.7426 C (μmol · L^{-1}) - 0.1067 (1.0–20 μmol · L^{-1}, R = 0.9991) and I_{pa} (μA) = 0.4032 C (μmol · L^{-1}) + 15.41 (20–120 μmol · L^{-1}, R = 0.9993) with a LOD of 33 nmol · L^{-1}. The sensitivities are 9.06 μA · μM^{-1} · cm^{-2} for HQ and 6.32 μA · μM^{-1} · cm^{-2} for CC, respectively. The relative standard deviations (RSDs) were 5.63% (1.0 μmol · L^{-1}) for HQ and 4.37% for CC (1.0 μmol · L^{-1}) by successive 7 measurements, respectively, indicating excellent repeatability of the modified electrode. The electrode has no significant change in peak potential and peak current after continuous 30 cycles. Also, when the electrode was stored at room temperature for about two weeks, the peak currents of 10.0 μmol · L^{-1} HQ and 10.0 μmol · L^{-1} CC decreased merely 3.82% for HQ and 4.21% for CC (n = 3), respectively, which shows long-term stability of the Fe/PC materials. A comparison of the present method with other electrochemical methods is listed in Table 1. It is clear that the present sensor is superior in some cases when compared to other reported electrode
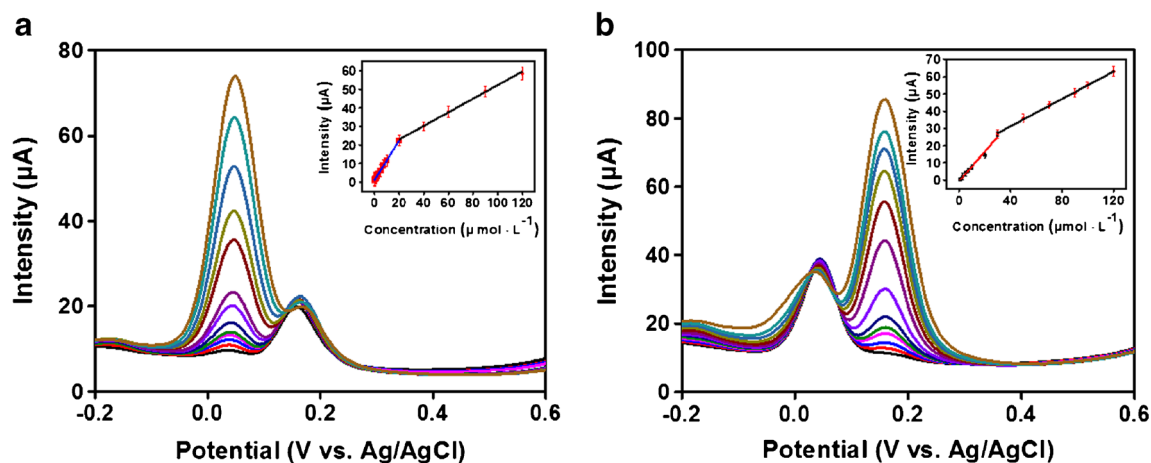

Fig. 2 Cyclic voltammograms of 10.0 μmol · L^{-1} HQ and 10.0 μmol · L^{-1} CC at the (a) bare GCE, (b) PC/GCE and (c) Fe/PC/GCE. Scan rate: 100 mV · s^{-1}

Fig. 3 Differential pulse voltammograms of a binary mixture of 10.0 μmol · L^{-1} CC and different concentrations of HQ (0.1–120 μmol · L^{-1}) at Fe/PC/GCE in phosphate buffer (pH 7.0) (**a**) Differential pulse voltammograms of a binary mixture of 10.00 μmol · L^{-1} HQ and different concentrations of CC (1–120 μmol · L^{-1}) at Fe/PC/GCE in phosphate buffer (pH 7.0) (**b**). The inserts were the relationships between the peak currents and concentrations

materials [4, 6, 7, 24–29]. The high sensitivity originates from a synergistic effect of nitrogen doping and iron species in porous carbon and its beneficial structure characteristics (high surface area and porous structure). These results also suggest that the modified electrode displays excellent selectivity for the determination of HQ and CC without mutual interference.

Interference study and real sample analysis

Different ions and compounds often coexist with HQ and CC in environmental water samples. Therefore, several nontarget water constituents were chosen to investigate their effect on HQ and CC detection. The results showed that 500-fold of K^+, Na^+, Ca^{2+}, and Mg^{2+}, 250-fold of Cl^-, SO_4^{2-}, NO_2^-, $H_2PO_4^-$, HPO_4^{2-}, and NO_3^-, 100-fold of Cu^{2+}, Zn^{2+}, and Pb^{2+}, 50-fold

uric acid, ascorbic acid, glucose, and hydrogen peroxide, rutin, quercetin, dopamine, triethanolamine, baicalin, hydroxylamine, and morin, 3-fold of resorcinol, bisphenol A, and p-nitrophenol did not interfere with HQ and CC determination (the peak current signal change below ±5%). This reflectes that the Fe/PC/GCE electrode has a wonderful selectivity for simultaneous detection of HQ and CC without impact from the common interfering substances.

The validity and practical application was examined by the measurement of HQ and CC concentration in the tap and lake water samples (Table 2). The recovery ranges were calculated to 100.1–102.0% for HQ and 97.0–101.1% for CC, respectively. The results illustrates that the present method shows excellent reliability and practicality for the simultaneous analysis in real samples.

Table 1 Performance comparison of Fe/PC/GCE for simultaneous determination of HQ and CC with other reported electrode materials

Electrode[a]	Linear range (μmol · L^{-1})		Detection limit (μmol · L^{-1})		Ref.
	HQ	CC	HQ	CC	
ZnS/NiS@ZnS/L-Cys/AuNPs/GCE	0.1–300	0.5–400	0.024	0.071	4
PME/GR-CPE	7.0–1000	–	0.074	–	6
GO/PM/GCE	–	0.03–138	–	0.008	7
CoPC-PGE	0.5–100	0.5–100	0.338	0.340	24
Cu-MOF-199/SWCNTs/GCE	0.1–1453	0.1–1150	0.08	0.1	25
pMA/EG/GCE	0.3–100	0.2–100	0.085	0.080	26
Pt/ZrO$_2$−RGO/GCE	1–1000	1–400	0.4	0.4	27
LRG/GCE	1–300	3–300	0.5	0.8	28
CNCs-RGO/GCE	1–400	1–300	0.87	0.4	29
Fe/PC/GCE	0.1–120	1–120	0.014	0.033	This work

[a] L-Cys: L-cysteine; PME/GR: poly(melamine)/graphene; PM: polymelamine; CoPC: cobalt-phtalocyanine; SWCNTs: single-walled carbon nanotubes; pMA/EG: poly- mercaptoacetic acid/exfoliated grapheme; RGO: Graphene oxide; LRG: reduced graphene; CNCs: carbon nanocages

Table 2 Recoveries for the determination of HQ and CC in tap and lakewater samples ($n = 3$)

Sample	Analyte	Added (μmol · L^{-1})	Founded (μmol · L^{-1})	Recovery (%)
Tap water	HQ	0.00	–	
		1.00	1.02	102.0
		20.00	20.03	100.1
	CC	0.00	–	
		1.00	0.97	97.0
		20.00	20.04	100.2
Lake water	HQ	0.00	–	
		1.00	1.01	101.0
		20.00	20.12	100.6
	CC	0.00	–	
		1.00	0.98	98.0
		20.00	20.23	101.1

Conclusion

In summary, MOFs derived iron species doped porous carbon as sensing materials has been prepared for the simultaneous detection of phenolic compounds. The HQ and CC can well be separated from each other with a large peak potential difference. The satisfactory results are obtained for the determination of the HQ and CC in the environmental water samples, which broadens the application of the MOFs materials in the analytical fields. However, this work also has some limitation. For example, the synthetic process of porous carbons derived from ZIF-8 is more complicated than other materials (grapheme, carbon nanotubes, and porous carbon spheres), and the morphology is affected by carbonization temperature and carbonization environment (nitrogen or air). Hence, we hope we can simplify the synthesis process without losing its analytical performance in the next work.

Compliance with ethical standards The authors declare that they have no competing interests.

References

1. Zhao GH, Li MF, ZH H, Li HX, Cao TC (2006) Electrocatalytic redox of hydroquinone by two forms of L-proline. J Mol Catal A 255:86–91
2. Hirakawa K, Oikawa S, Hiraku Y, Hirosawa I, Kawanishi S (2002) Catechol and hydroquinone have different redox properties responsible for their differential DNA-damaging ability. Chem Res Toxicol 15:76–82
3. Yao XT, Wen LQ, Rong SY, Ying LQ (2006) Simultaneous determination of positional isomers of benzenediols by capillary zone electrophoresis with square wave amperometric detection. J Chromatogr A 1109:317–321
4. Wang Y, JH Q, Li SF, Dong Y, JY Q (2015) Simultaneous determination of hydroquinone and catechol using a glassy carbon electrode modified with gold nanoparticles, ZnS/NiS@ZnS quantum dots and L-cysteine. Microchim Acta 182:2277–2283
5. Liu LY, Ma Z, Zhu XH, Alshahrani LA, Tie SL, Nan JM (2016) A glassy carbon electrode modified with carbon nano-fragments and bismuth oxide for electrochemical analysis of trace catechol in the presence of high concentrations of hydroquinone. Microchim Acta 183:3293–3301
6. Peng J, Feng Y, Han XX, Gao ZN (2016) Simultaneous determination of bisphenol A and hydroquinone using a poly(melamine) coated graphene doped carbon paste electrode. Microchim Acta 183:2289–2296
7. Palanisamy S, Ramaraj SK, Chen SM, Velusamy V, Yang TCK, Chen TW (2017) Voltammetric determination of catechol based on a glassy carbon electrode modified with a composite consisting of graphene oxide and polymelamine. Microchim Acta 184:1051–1057
8. Huang KJ, Wang L, Li J, Yu M, Liu YM (2013) Electrochemical sensing of catechol using a glassy carbon electrode modified with a composite made from silver nanoparticles, polydopamine, and graphene. Microchim Acta 180:751–757
9. Ma XM, Liu ZN, Qiu CC, Chen T, Ma HY (2013) Simultaneous determination of hydroquinone and catechol based on glassy carbon electrode modified with gold-graphene nanocomposite. Microchim Acta 180:461–468
10. Aiyappa HB, Pachfule P, Banerjee R, Kurungot S (2013) Porous carbons from nonporous MOFs: influence of ligand characteristics on intrinsic properties of end carbon. Cryst Growth Des 13:4195–4199
11. Cheng Q, Ji LD, KB W, Zhang WK (2016) Morphology-dependent electrochemical enhancements of porous carbon as sensitive determination platform for ascorbic acid, dopamine and uric acid. Sci Report 6:22309
12. Lim DW, Yoon JW, Ryu KY, Suh MP (2012) Magnesium nanocrystals embedded in a metal-organic framework: hybrid hydrogen storage with synergistic effect on physi- and chemisorption. Angew Chem Int Ed 51:9814–9817
13. Torad NL, Hu M, Kamachi Y, Takai K, Imura M, Naito M, Yamauchi Y (2013) Facile synthesis of nanoporous carbons with controlled particle sizes by direct carbonization of monodispersed ZIF-8 crystals. Chem Commun 49:2521–2523
14. Tang HL, Cai SC, Xie SL, Wang ZB, Tong YX, Pan M, XH L (2016) Metal-organic-framework-derived dual metal- and nitrogen-doped carbon as efficient and robust oxygen reduction reaction catalysts for microbial fuel cells. Adv Sci 3:1500265
15. Wang ZF, Liu YS, Gao CW, Jiang H, Zhang JM (2015) A porous Co(OH)$_2$ material derived from a MOF template and its superior energy storage performance for supercapacitors. J Mater Chem A 3:20658–20663
16. Horcajada P, Chalati T, Serre C, Gillet B, Sebrie C, Baati T, Eubank JF, Heurtaux D, Clayette P, Kreuz C, Chang JS, Hwang YK, Marsaud V, Bories PN, Cynober L, Gil S, Férey G, Couvreur P, Gref R (2010) Porous metal-organic-framework nanoscale carriers as a potential platform for drug delivery and imaging. Nat Mater 9:172–178
17. Krokidas P, Castier M, Moncho S, Brothers E, Economou IG (2015) Molecular simulation studies of the diffusion of methane, ethane, propane, and propylene in ZIF-8. J Phys Chem C 119:27028–27037

18. Karagiaridi O, Lalonde MB, Bury W, Sarjeant AA, Farha OK, Hupp JT (2012) Opening ZIF-8: a catalytically active zeolitic imidazolate framework of sodalite topology with unsubstituted linkers. J Am Chem Soc 134:18790–18796

19. Gualino M, Roques N, BrandèS SP, Arurault L, Sutter JP (2015) From ZIF-8@Al_2O_3 composites to self-supported ZIF-8 one-dimensional superstructures. Cryst Growth Des 15:3552–3555

20. Wang XJ, Zhang HG, Lin HH, Gupta S, Wang C, Tao ZX, Fu H, Wang T, Zheng J, Wu G, Li XG (2016) Directly converting Fe-doped metal–organic frameworks into highly active and stable Fe-N-C catalysts for oxygen reduction in acid. Nano Energy 25:110–119

21. Almasoudi A, Mokaya R (2012) Preparation and hydrogen storage capacity of templated and activated carbons nanocast from commercially available zeolitic imidazolate framework. J Mater Chem 22:146–152

22. Liu T, Zhao PP, Hua X, Luo W, Chen SL, Cheng GZ (2016) An Fe–N–C hybrid electrocatalyst derived from a bimetal–organic framework for efficient oxygen reduction. J Mater Chem A 4:11357–11364

23. Wang ZH, Qie L, Yuan LX, Zhang WX, XL H, Huang YH (2013) Functionalized N-doped interconnected carbon nanofibers as an anode material for sodium-ion storage with excellent performance. Carbon 55:328–334

24. Buleandra M, Rabinca AA, Badea IA, Balan A, Stamatin I, Mihailciuc C, Ciucu AA (2017) Voltammetric determination of dihydroxybenzene isomers using a disposable pencil graphite electrode modified with cobalt-phthalocyanine. Microchim Acta 184:1481–1488

25. Zhou J, Li X, Yang LL, Yan SL, Wang MM, Cheng D, Chen Q, Dong YL, Liu P, Cai WQ, Zhang CC (2015) The Cu-MOF-199/single-walled carbon nanotubes modified electrode for simultaneous determination of hydroquinone and catechol with extended linear ranges and lower detection limits. Anal Chim Acta 899:57–65

26. Fu J, Tan XH, Shi Z, Song XJ, Zhang SH (2016) Highly sensitive and simultaneous detection of hydroquinone and catechol using poly(mercaptoacetic acid)/exfoliated graphene composite film-modified electrode. Electroanalysis 28:203–210

27. Ezhil Vilian AT, Chen SM, Huang LH, Ali MA, Al-Hemaid FMA (2014) Simultaneous determination of catechol and hydroquinone using a Pt/ZrO_2-RGO/GCE composite modified glassy carbon electrode. Electrochim Acta 125:503–509

28. Lai T, Cai WH, Dai WL, Ye JS (2014) Easy processing laser reduced graphene: a green and fast sensing platform for hydroquinone and catechol simultaneous determination. Electrochim Acta 138:48–55

29. Huang YH, Chen JH, Sun X, ZB S, Xing HT, SR H, Weng W, Guo HX, WB W, He YS (2015) One-pot hydrothermal synthesis carbon nanocages-reduced graphene oxide composites for simultaneous electrochemical detection of catechol and hydroquinone. Sensors Actuators B Chem 212:165–173